

# Changes in Microstructure of Air Plasma Sprayed M-CrAlY Coatings After Short Thermal Exposure in Argon Atmosphere

L. ČELKO<sup>a,\*</sup>, V. ŘIČÁNKOVÁ<sup>a</sup>, L. KLAKURKOVÁ<sup>a</sup>, T. PODRÁBSKÝ<sup>a</sup>, E. DVOŘÁČEK<sup>b</sup>  
AND J. ŠVEJCAR<sup>a</sup>

<sup>a</sup>Institute of Materials Science and Engineering, Faculty of Mechanical Engineering, Brno University of Technology  
Technická 2, Brno 616 69, Czech Republic

<sup>b</sup>S.A.M. — Metallizing Company, Ltd., Hájecká 12, Brno, 618 00, Czech Republic

Conventional air plasma spray technique and two powders, NiCrAlY and CoNiCrAlY, were used to produce the M-CrAlY type of coating on the Inconel 713LC substrate. Two phase coatings, consisting of Ni and/or Co solid solution and NiAl intermetallic phase, were produced. A certain amount of imperfectly melted powder particles, voids and aluminium oxide was also present. After air plasma spraying the coatings were annealed at widely ranging temperatures (650, 800, 1000 and 1150 °C) for two hours in argon-flow atmosphere. It was found that the temperature significantly affects the microstructure of resulting coatings. The oxide scale was formed by internal oxidation in a coating region primarily at higher temperatures. In this case, aluminium was depleted from the NiAl phase within the coating region and the Ni, Co, Cr solid solutions and the aluminium oxide started to form rapidly. No interaction was observed after the short thermal exposure below the substrate surface. The microstructure of coatings was recorded by scanning electron microscope. Coating thickness, amount of voids and oxide scale were measured by means of image analysis. The concentration of phases was estimated by energy dispersive microanalysis.

PACS: 81.15.Rs

## 1. Introduction

Superalloys, most reliable and cost-effective alloys in terms of resisting high operating temperature and stress levels, have been developed for components working in both high-temperature and high-pressure sections of aircraft and industrial gas turbines [1]. Therefore, in accordance with the relationship between the low purchase costs, good corrosion and oxidation resistance, and excellent creep and fatigue strengths, the cast polycrystalline nickel-base superalloy Inconel 713 LC is the subject of extensive studies [2, 3].

To protect the superalloy surface against detrimental oxidation and corrosion processes, a specific group of high-temperature coatings were designed in the last five decades. For example, metal-based aluminide diffusion coatings and M-CrAlY overlay coatings are most widely used [4–6]. The M-CrAlY coating types (where M = Ni, Co, Fe or their appropriate mutual combination) are utilized on parts as standalone coatings and as bond coats for thermal barrier coating systems [7]. The structure and properties of these coatings can in principle be influenced by chemical composition and manufacturing technology.

In the field of chemical composition, small additions of Re, Hf, CeO<sub>2</sub>, rare earths and other compounds to the M-CrAlY coatings were studied. It was found that Re increases the stability and enhances the  $\alpha$ -Cr phase precipitation in the coating during oxidation. Overall, it promotes better adhesion and reduces thermal stresses at the coating-substrate interface [8]. On the other hand, CeO<sub>2</sub> additions in the M-CrAlY coatings provide a reduction by more than one third of the weight gain in comparison with bare superalloys [9].

The coating thickness and density, preferred grain size and orientation, porosity and surface roughness are considered as the most technologically important parameters which in the end affect the deposited coating characteristics. These can also be influenced by an appropriate design of deposition technology. In practice, the most widely used techniques for producing M-CrAlY coatings are the electron-beam, electric-arc and plasma methods. As regards the plasma spray methods, the air plasma spray (APS), low pressure plasma spray (LPPS), vacuum plasma spray (VPS), and high velocity oxyfuel (HVOF) techniques can be chosen. The coating microstructure appearance resulting from these plasma methods differs primarily in unmelted particles, porosity and oxide scale quantity. The cost of coating deposition by these techniques is relatively low but their use is limited to relatively simple-shaped parts. Moreover, the laser-beam,

\* corresponding author; e-mail: celko@fme.vutbr.cz

electron-beam and spark plasma sintering techniques can also be used to enhance the coating properties via remelting the coating surface [10–12].

When the M-CrAlY coatings are exposed to high temperatures, the thermally grown oxide (TGO) scale starts to form by interaction with oxidizing atmosphere. The knowledge of the degradation processes, phase transformations, reaction kinetics and nature of the oxide scale formation in these coatings is important for their use in applied practice to ensure the slow growing TGO scale during oxidation. For this reason isothermal oxidation tests are extensively applied [13–16].

In the present study, the changes in microstructure of air plasma sprayed coatings from two commercially available NiCrAlY and CoNiCrAlY powders were studied in a wide temperature range (650–1150 °C). Only short dwells in argon-flow atmosphere were applied with the aim of reducing the interactions caused by oxygen from the surrounding environment. The phases transformation originated by inward and outward diffusion of reactive elements and by increased porosity content within the inner coating region were investigated.

## 2. Experimental

Commercially available nickel-base superalloy Inconel 713LC (PBS Velká Bíteš, a.s., Czech Republic) was used as the substrate material. Cylinder (30 × 10 mm) surface was ground with abrasive paper down to #600, polished with 3 µm diamond paste and washed with acetone before the coating deposition. Two powders, NiCrAlY with nominal particle size 38–53 and CoNiCrAlY with 45–65 µm (GTV GmbH, Germany), were sprayed onto the substrate surface using the air plasma spray technique. The average thickness of the sprayed coatings was about 125 µm for M-CrAlY and 65 µm for CoNiCrAlY. Nominal composition of the substrate and the powders is listed in Table I.

TABLE I

Nominal composition of the substrate and the powders [wt.%]

	C	Al	Nb	Ti	Cr	Ni	Co	Mo	Y
Substrate									
Inconel 713LC	0.2	12.1	1.2	0.9	12.7	bal.			2.6
Powder									
NiCrAlY		19.0			21.7	bal.			0.6
CoNiCrAlY		15.6			21.2	27.7	bal.		0.3

Specimens for microstructure characterization were heated at 650, 800, 1000 and 1150 °C for 2 hrs in a Heraeus tube furnace with flowing argon atmosphere. After the short isothermal heat treatment the specimens were cooled in argon-flow atmosphere down to the room temperature.

For microstructure observation, a Philips XL30 scanning electron microscope (SEM) was used. The chemical composition was estimated using an energy dispersive X-Ray spectrometer EDAX (EDS) attached to the SEM. Measurements of layer thickness, voids and aluminium oxide scale were performed on at least three independent regions from SEM images by means of the NIS Elements AR 2.3 image analysis.

## 3. Results and discussion

### 3.1. As-sprayed coating microstructure

The initial state of the plasma sprayed NiCrAlY and CoNiCrAlY coatings shows a typical microstructure in accordance with the technology used. The microstructure is primarily composed of flattened remelted powder particles and an adequate quantity of porosity, unmelted particles and oxide scale, as shown by observation of cross-sectioned samples printed in Fig. 1.

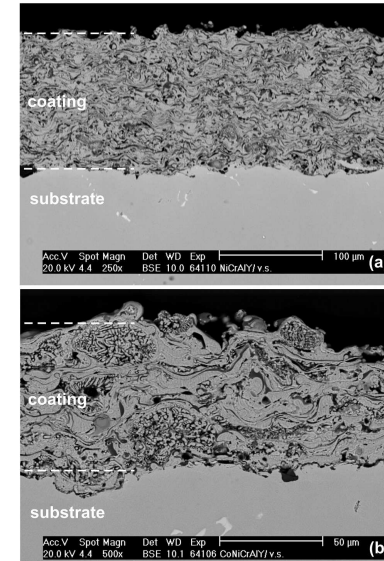


Fig. 1. SEM backscattered electron images of (a) NiCrAlY and (b) CoNiCrAlY coatings on Inconel 713 LC: As-sprayed state.

Generally, the plasma sprayed M-CrAlY coatings consist of two major phases:  $\gamma$ -Ni and/or Co solid solution and  $\beta$ -NiAl and/or CoAl intermetallic phase. The  $\gamma'$ -Ni<sub>3</sub>Al phase and the  $\alpha$ -Al<sub>2</sub>O<sub>3</sub> were identified as minority phases. External porosity and no apparent inter-diffusion layer were observed at the coating – substrate interface.

### 3.2. Changes in microstructure with exposure time

The microstructure of NiCrAlY and CoNiCrAlY coatings after annealing at a temperature of 650 °C is shown in Fig. 2. There are no significant changes apparent in comparison with the microstructure of as-sprayed coatings. Based on the EDX measurements performed (Table

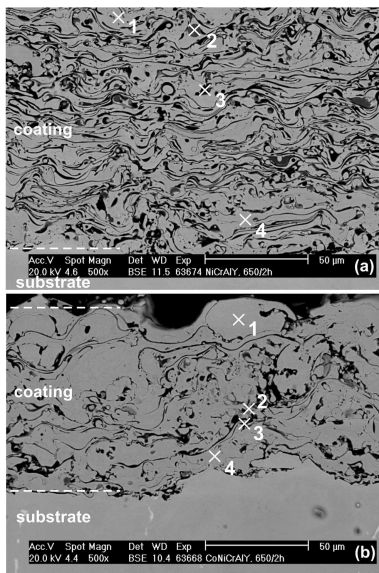


Fig. 2. SEM backscattered electron images of (a) NiCrAlY and (b) CoNiCrAlY coatings on Inconel 713 LC: 650°C/2 hrs (Ar).

II) and on the knowledge of phase stoichiometry, several phases within the coating regions can be expected. These are Ni-Cr and (Co, Ni)-Cr solid solutions (points 1 – NiCrAlY and 4 – CoNiCrAlY), NiAl, CoAl, and Ni<sub>3</sub>Al intermetallics (points 4 – NiCrAlY and 1, 2 – CoNiCrAlY) and alumina or complex aluminum based oxides (points 2, 3 – NiCrAlY and 3 – CoNiCrAlY).

TABLE II

Results from SEM/EDS analyses indicated in Fig. 2 [at.%]: 650°C/2 hrs (Ar).

	NiCrAlY				CoNiCrAlY			
	1	2	3	4	1	2	3	4
O	16.4	63.1	56.5	4.1	6.8	4.0	48.2	4.4
Al	6.9	15.7	35.3	18.8	21.5	39.8	29.3	11.7
Cr	18.5	13.6	2.5	20.4	17.0	14.0	6.0	21.2
Ni	58.2	7.0	4.3	56.7	27.5	18.5	7.5	30.3
Co					27.2	23.7	8.0	32.4
Y	0.6	1.4				1.0		

The most significant changes occurring in the microstructure of analyzed coatings can be observed in the temperature range from 1000 to 1150 °C, see Fig. 3. At the coating-substrate and flattened particles interfaces the amount of dark-grey phase increases.

The EDX analyses listed in Table III show that the dark-grey phase consists of high content of oxygen and aluminium, and their content corresponds to the Al<sub>2</sub>O<sub>3</sub> compound stoichiometry (points 7, 8 and 9 – NiCrAlY and 7 – CoNiCrAlY). In contrast to the argon-flow atmosphere applied to reduce the oxygen content, the alu-

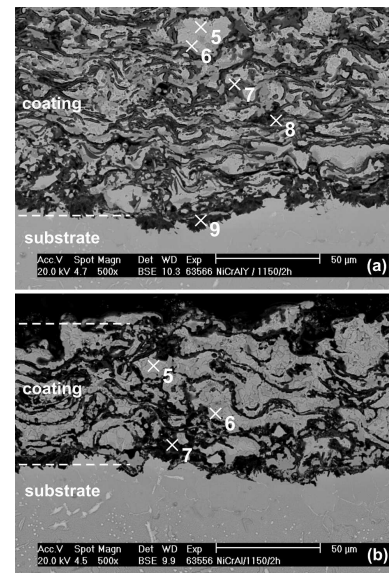


Fig. 3. SEM backscattered electron images of (a) NiCrAlY and (b) CoNiCrAlY coatings on Inconel 713 LC: 1150°C/2 hrs (Ar).

minium oxide scale was formed. Moreover, inside the flattened particles, the concentration of Ni-Cr and (Co, Ni)-Cr solid solutions (points 5 – NiCrAlY, CoNiCrAlY) and α-Cr phase (points 6 – NiCrAlY and CoNiCrAlY) was only estimated. When compared with lower annealing temperatures, no intermetallic phases were found after annealing at 1150 °C. The depletion of aluminum from the intermetallics absorbed during the oxide scale formation causes their irreversible transformation into the aluminum-free or aluminum-reduced Ni(Co)-Cr solid solutions and/or α-Cr regions. Some results of isothermal oxidation studies [14, 15] also show that the Ni or Co outward diffusion and solid-state reactions with pre-existing aluminum oxide enable the formation of Al<sub>2</sub>O<sub>3</sub> and Cr<sub>2</sub>O<sub>3</sub> protective oxide scale.

TABLE III

Results from SEM/EDS analyses as indicated in Fig. 3 [at.%]: 1150°C/2 hrs (Ar)

	5	6	7	8	9	5	6	7
O	1.6	2.3	61.4	42.1	55.4	4.3	8.2	58.7
Al			30.2	34.0	41.8		1.7	37.6
Cr	10.3	93.6	1.2	2.7	1.8	10.7	60.2	1.2
Ni	88.1	4.1	6.3	19.6	1.0	44.4	9.3	1.7
Co						40.6	20.6	0.8
Y			0.9	1.6				

### 3.3 Voids and oxide formation

Oxidation caused by oxygen present in the surrounding argon atmosphere can be, to a great extent, eliminated

because of no substantial change in the coating thickness was found after annealing at the widely ranging temperatures, see Fig. 4a.

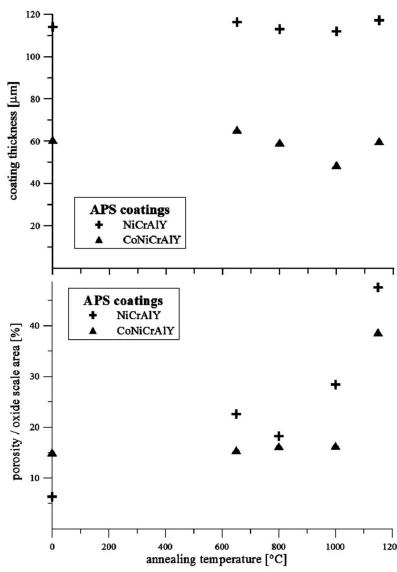


Fig. 4. The changes in NiCrAlY and CoNiCrAlY coatings (a) thickness and (b) porosity/oxide scale area.

In contrast to the coating thickness, the amount of voids and/or oxide scale in the inner coating region increases, see Figure 4b. Both studied coatings exhibit different behavior of voids and/or different oxide scale formation. The NiCrAlY coatings show a gradual increase in their formation with increasing temperature. On the other hand, the amount of the voids and/or oxide scale in the case of CoNiCrAlY coatings remains stable up to 1000 °C and then sharply increases at a temperature of 1000–1150 °C. It was shown that from these two coating types the NiCrAlY coating also exhibited more than 10% higher deviation. The results obtained after the short isothermal annealing are in contrast with the long-term isothermal oxidation tests [11], where only a slight decrease in these parameters was observed.

#### 4. Conclusion

The most significant changes in coating microstructures were apparent in the temperature range of 1000–1150 °C. Whereas the NiCrAlY coating porosity/oxide scale grows slightly with increasing temperature, the CoNiCrAlY coating porosity/oxide scale remains up to a temperature of 1000 °C and then grows markedly in the

range from 1000 to 1150 °C. After annealing at temperatures of 1000 and 1150 °C the aluminum depletion from the inner region of splats was observed. Two-phase regions  $\gamma$ -(Ni,Co) +  $\beta$ -(NiAl) transform into the  $\gamma$ -(Ni,Co) +  $\alpha$ -(Cr) + alumina. The CoNiCrAlY coating was found to be more stable in combination with the IN 713LC substrate alloy.

#### Acknowledgments

The authors acknowledge the financial support for this work provided by the Ministry of Education, Youth and Sports Research Plan No. MSM 0021630508 and the Ministry of Industry and Trade Project No. FR – TI1/099.

#### References

- [1] M.J. Donachie, S.J. Donachie, *Superalloys – A Technical Guide*, ASM International, Ohio 2002).
- [2] M. Petrenec, K. Obrtlik, J. Polak, *Key Eng. Mater.* **348-349**, 101 (2007).
- [3] M. Juliš, K. Obrtlík, S. Pospíšilová, T. Podrábský, J. Polák, *Procedia Engineering* **2**, 1983 (2010).
- [4] Y. Tamarin, *Protective Coatings for Turbine Blades*, ASM International, Ohio 2002.
- [5] T. Bose, *High Temperature Coatings*, Elsevier, Oxford 2007.
- [6] L. Čelko, L. Klakurková, O. Man, J. Švejcar, *Mater. Manufact. Process.* **24**, 1155 (2009).
- [7] T. Patterson, A. Leon, B. Jayaraj, J. Liu, Y.H. Sohn, *Surf. Coat. Technol.* **203**, 437 (2008).
- [8] L. Huang, X.F. Sun, H.R. Guan, Z.Q. Hu, *Surf. Coat. Technol.* **201**, 1421 (2006).
- [9] R.A. Mahesh, R. Jayaganthan, S. Prakash, *Mater. Chem. Phys.* **119**, 449 (2010).
- [10] U. Dragos, M. Gabriela, B. Waltraut, C. Ioan, *Solid State Sci.* **7**, 459 (2005).
- [11] D. Seo, K. Ogawa, M. Tanno, T. Shoji, S. Murata, *Surf. Coat. Technol.* **201**, 7952 (2007).
- [12] D. Oquab, C. Estournes, D. Monceau, *Adv. Eng. Mater.* **9**, 413 (2007).
- [13] M.C. Mayoral, J.M. Andrés, M.T. Bona, V. Higuera, F.J. Belzunce, *Surf. Coat. Technol.* **202**, 1816 (2008).
- [14] Weizhou Li, Yueqiao Li, Chao Sun, Zhiliu Hu, Tianquan Liang, Wuquan Lai, *J. Alloys Compd.* (2010), **506**, 77 (2010).
- [15] F.H. Yuan, Z.X. Chen, Z.W. Huang, Z.G. Wang, S.J. Zhu, *Corros. Sci.* **50**, 1608 (2008).
- [16] J. Toscano, A. Gil, T. Hüttel, E. Wessel, D. Naumenko, L. Singheiser, W.J. Quadakkers, *Surf. Coat. Technol.* **202**, 603 (2007).